Macromolecules

ARTICLE

pubs.acs.org/Macromolecules

Controlling the Dynamics of Self-Assembled Triblock Copolymer Networks via the pH

Céline Charbonneau, Christophe Chassenieux,* Olivier Colombani,* and Taco Nicolai

LUNAM Université, Laboratoire Polymères, Colloïdes et Interfaces, UMR CNRS 6120 - Université du Maine, av. O. Messiaen, 72085 Le Mans cedex 9, France

ABSTRACT: Triblock copolymers were synthesized by ATRP with a poly(acrylic acid) (PAA) central block and random copolymer end blocks containing both AA and *n*-butyl acrylate (*n*BA) units. Self-assembly in aqueous solution was investigated over a wide range of concentrations. The degree of ionization of the AA units (α) was varied between 0.1 and 0.9 by varying the pH. The dynamic mechanical properties of the systems were investigated using oscillatory shear measurements. With increasing pH a transition from frozen hydrogels to dynamic networks was observed at pH = 5.2 (α = 0.30). The dynamic polymer networks behaved as viscoelastic liquids with a terminal relaxation time that decreased over 7 decades with increasing pH. This remarkable feature enables fine-tuning and control of the rheology.

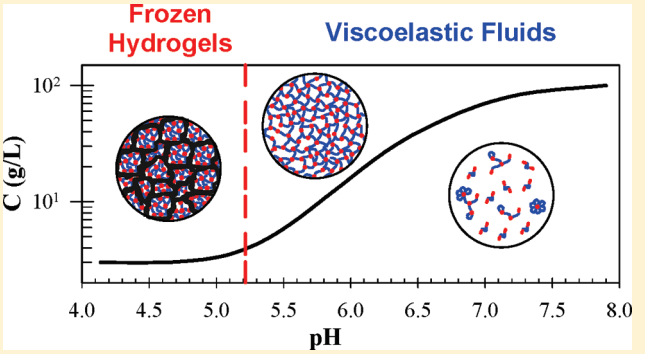

I. INTRODUCTION

Triblock copolymers of BAB type self-assemble into multiplets when dissolved in a selective solvent for block A. The properties of these systems have been investigated extensively in the past and are well understood when the association is dynamic.[1−6] We will briefly review this situation first. The multiplets are constituted of a dense core containing n_a B blocks surrounded by a corona of solvated A blocks. In highly diluted solutions, the chains form loops and the multiplets are flowerlike. When the concentration is increased, the B blocks of a single chain may enter the cores of two different multiplets which become bridged by an A block. With increasing concentration the multiplets connect into larger aggregates until at a critical percolation concentration (C_p) a space spanning network is formed[7−9] (see Figure 1). As a consequence, the viscosity rises sharply with increasing concentration above C_p, but it does not diverge because the bonds break and re-form spontaneously.

The rheological properties of the transient network depend on both the amount and the lifetime of the bridges. The high-frequency elastic shear modulus (G_e) is well described by the theory of rubber elasticity at least if the bridging chains are flexible and not entangled.[10] Mechanical strain relaxes by the spontaneous exchange of B blocks between multiplets and the relaxation is often characterized by a single relaxation time so that the frequency dependence can be well described by the Maxwell equation. If the relaxation time is very long, the solution behaves like a gel. The chemical nature of both blocks has been varied in order to control the exchange rate of the B blocks between multiplets. Dynamic self-assembly with fast exchange rates are found when the B blocks are very short[5,11,12] or not very solvophobic.[13−15]

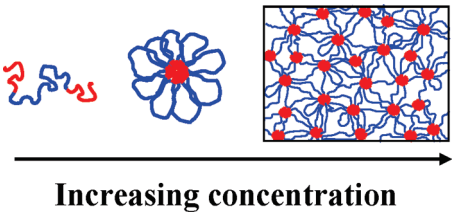

Figure 1. Schematic drawing of the aggregation of associating polymers. The associating blocks B are red, and the solvophilic block A is blue.

The description given above is valid only if the self-assembly is dynamic. However, for many systems the exchange rate is imperceptibly small and the systems are kinetically frozen.[16−20] In the case of triblock copolymers, absence of exchange may lead to the formation of gels that display no viscoelasticity and whose properties depend on the preparation method.[21−24] For such systems the viscosity is found to become immeasurably large above a critical concentration. The frozen character of block copolymers can be explained by the fact that the energy barrier that needs to be overcome for a block to escape from the core is $E \propto N^{2/3}\gamma$, where N is the polymerization degree of the B block and γ its surface tension with respect to the solvent.[25] In aqueous solutions the high value of γ for typical hydrophobic blocks such

Received: February 2, 2011
Revised: April 20, 2011
Published: May 12, 2011

as polystyrene or poly(*n*-butyl acrylate) prevents any exchange between the multiplets even for small values of N.[26,27]

One way to decrease γ is to incorporate solvophilic units within the solvophobic blocks as was reported earlier by our research group for diblock copolymers based on acrylic acid (AA) and *n*-butyl acrylate (*n*BA).[28,29] When dissolved in water, P(nBA$_{50\%}$-*stat*-AA$_{50\%}$)$_{99}$-*b*-PAA$_{98}$, containing 50% AA units in the moderately hydrophobic block, forms polymeric micelles whose aggregation number varies reversibly with varying pH,[29] whereas PnBA$_{90}$-*b*-PAA$_{100}$, consisting of a pure P*n*BA hydrophobic block, forms frozen aggregates.[30] pH-dependent self-assembly was also reported for so-called bis-hydrophilic diblock copolymers for which one of the blocks becomes solvophobic when the pH is changed.[31−33]

Here we report an investigation of triblock copolymers with a pure poly(acrylic acid) (PAA) A block and B blocks that contained both hydrophobic *n*-butyl acrylate and hydrophilic acrylic acid units incorporated in a controlled manner. In water, these polymers form viscoelastic liquids or hydrogels. The objective of this study was to demonstrate that including acidic units into the hydrophobic block renders the system dynamic in a controlled manner and allows control of the rheology via the pH. The viscoelastic properties of the networks will be discussed in detail as a function of the ionization degree and the polymer concentration, and we will show how they can be easily tuned by varying the pH. Our investigation demonstrates that dynamic mechanical measurements are a convenient way to determine the exchange rate of self-assembled block copolymers and to establish whether they are equilibrated or kinetically frozen.

II. MATERIALS AND METHODS

1. Materials. *n*-Butyl acrylate (*n*BA) and *tert*-butyl acrylate (*t*BA) (Acros, 99%) were stirred overnight with hydroquinone (Prolabo) on calcium hydride (Acros, 93%) and distilled under vacuum. Copper bromide (CuBr, Acros, 98%) was stirred overnight in glacial acetic acid (CH_3COOH, Aldrich, 99.7%), filtered, and rinsed successively with acetic acid, ethanol, and ether to remove traces of $CuBr_2$. *N,N,N′,N′,N″*-Pentamethyldiethylenetriamine (PMDETA, Acros, 99%), dimethyl 2,6-dibromoheptandioate (DMDBHD, Aldrich, 97%), acetone (Aldrich, 99.5%), copper(II) bromide ($CuBr_2$, Acros, 99%), *n*-decane (Acros, 99%), SiO_2 (63−200 μm, Fluka, chromatography grade), chloroform (Aldrich, 99.8%), methanol (Aldrich, 99%), trifluoroacetic acid (CF_3COOH, Acros, 99%), dichloromethane (Aldrich, 99.5%), sodium hydroxide (0.1 M, VWR; 1 M, Lab-online), and chlorhydric acid (1 M, VWR) were used as received.

2. Synthesis. For the bifunctional macroinitiator Br-P*t*BA$_{204}$-Br, Cu(II)Br$_2$ (0.044 g, 1.95×10^{-4} mol), PMDETA (0.71 g, 4.1×10^{-3} mol), and acetone (50 g) were introduced in a 500 mL round-bottom flask. After complete dissolution of the copper complex, *n*-decane (20 g), DMDBHD (1.34 g, 3.9×10^{-3} mol), and *t*BA (200 g, 1.56 mol) were added. The flask was closed with a screw cap equipped with a septum, and the solution was degassed by argon bubbling for 10 min. CuBr (0.56 g, 3.9×10^{-3} mol) was introduced in a second 500 mL round-bottom flask. The latter values correspond to the molar ratio [*t*BA]:[DMDBHD]:[CuBr]:[PMDETA] = 400:1:1:1.05. The flask was closed with a screw cap equipped with a septum and degassed by a flow of argon for 15 min. The content of the first flask was transferred in the second one under pressure of argon using a double-tipped needle. A few drops of the solution were taken as sample t_0, and the flask was dipped in an oil bath at 60 °C.

Samples were withdrawn throughout the reaction to follow the kinetics as reported elsewhere.[29,30] The conversion was determined by gas chromatography using *n*-decane as internal standard.[29,34] Number (M_n) and weight (M_w) averaged molar mass were determined after copper removal using size exclusion chromatography (SEC) in THF calibrated with polystyrene (PS) standards (see below). The reaction was stopped at 51% conversion by cooling the flask to 0 °C (ice−water) and opening it to air. The polymer was purified by column chromatography ($SiO_2/CHCl_3$) followed by precipitation in methanol/water (90/10 vol/vol), yielding a viscous yellowish liquid: M_n (calculated from the conversion) = 2.6×10^4 g/mol, M_n (SEC) = 2.4×10^4 g/mol, dispersity M_w/M_n (SEC) = 1.16.

For the triblock copolymer Br-P(nBA$_{50\%}$-*stat*-*t*BA$_{50\%}$)$_{101}$-*b*-P*t*BA$_{204}$-*b*-P(nBA$_{50\%}$-*stat*-*t*BA$_{50\%}$)$_{101}$-Br, a similar procedure was used with the following amounts of reagents: Cu(II)Br$_2$ (0.028 g, 1.25×10^{-4} mol), PMDETA (0.46 g, 2.6×10^{-3} mol), acetone (16.1 g), *n*-decane (6.5 g), Br-P*t*BA$_{204}$-Br (33.4 g, 1.26×10^{-3} mol), *t*BA (32.3 g, 2.52 × 10^{-1} mol), *n*BA (32.3 g, 2.53×10^{-1} mol), and Cu(I)Br (0.362 g, 2.53×10^{-3} mol). The latter values correspond to the molar ratio [*n*BA + *t*BA]:[DMDBHD]:[CuBr]:[PMDETA] = 400:1:2:2.10. The reaction was stopped at 50% conversion. M_n (calculated) = 5.2×10^4 g/mol, M_n (SEC) = 4.9×10^4 g/mol, dispersity M_w/M_n (SEC) = 1.10.

The Br-P(nBA$_{50\%}$-*stat*-*t*BA$_{50\%}$)$_{101}$-*b*-P*t*BA$_{204}$-*b*-P(nBA$_{50\%}$-*stat*-*t*BA$_{50\%}$)$_{101}$-Br triblock copolymer was dissolved in dichloromethane ($C \sim 150$ g/L) and stirred at room temperature for 48 h with 5 equiv of trifluoroacetic acid relative to the amount of *t*BA units.[30] The polymer was collected after rotating evaporation of the solvent and the trifluoroacetic acid. The elimination of the residual CF_3COOH was achieved by three cycles of redissolution in methanol/dichloromethane mixture (1/10 v/v), rotating evaporation, and vacuum pumping. ^{13}C NMR revealed the absence of significant quantities of residual trifluoroacetic acid after drying as already published for P*n*BA-*b*-PAA diblocks.[30]

3. Sample Preparation. Every sample was prepared independently using the following procedure. The quantity of NaOH required to reach the desired ionization degree of the AA units (α) was calculated from the chemical structure of the polymer and considering that all AA units could be ionized (as was verified by potentiometric titration). The polymer was dissolved in demineralized water (Millipore) containing the required amount of NaOH. The polymer solutions were homogenized while stirring during at least 1 day. The samples were degassed under vacuum for 3−5 min. This procedure led to homogeneous and perfectly transparent solutions except at higher concentrations and low α where the system remained a strong gel even at 80 °C. The difficulty to homogenize strong gels limited the range of concentrations that could be explored.

4. Methods. *4.1. Potentiometric titration* were performed at room temperature with an automatic titrator (TIM 856, Radiometer Analytical) controlled by the TitraMaster 85 software.

4.2. Dynamic mechanical measurements were carried out with two controlled-stress rheometers equipped with a cone−plate geometry: AR2000 (angle = 4°−1°−0.58°, diameter = 20−40−60 mm depending on the viscosity of the sample) and MCR301 (angle = 1°, diameter = 24 mm). To prevent water evaporation, the geometry was covered with silicon oil. The temperature was controlled with a Peltier system. Oscillatory shear measurements were done in the linear response regime. Samples were loaded onto the rheometer, and it was verified that the system was stable before the frequency dependence of the storage (G') and loss (G'') shear moduli was measured.

The viscosity of the solutions (η) was determined by oscillatory shear or by shear flow measurements. A controlled-speed rheometer (Low Shear 40) equipped with a Couette geometry (din 412) was used to determine the viscosity of solutions with low viscosities ($10^{-3} < \eta < 10^{-2}$ Pa·s). The temperature was controlled by a thermostated bath.

4.3. Size exclusion chromatography (SEC). was performed using a PL-gel Mixed C, 5 μm, 60 cm column with THF as eluent (flow rate = 1.0 mL/min), at room temperature, and using refractometry for detection (Shodex RI 71 refractometer, Showa Denko). The number-average

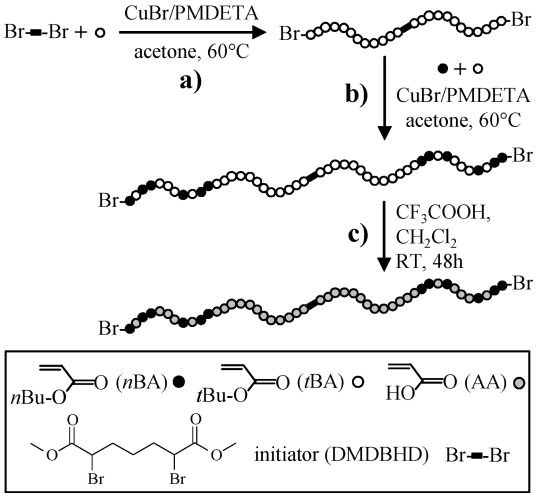

Figure 2. Steps of the polymerization of the P(nBA$_{50\%}$-*stat*-AA$_{50\%}$)$_{101}$-*b*-PAA$_{204}$-*b*-P(nBA$_{50\%}$-*stat*-AA$_{50\%}$)$_{101}$ triblock copolymer (TH50) by atom transfer radical polymerization (ATRP): (a) synthesis of the Br-PtBA$_{204}$-Br precursor, (b) synthesis of the P(nBA$_{50\%}$-*stat*-tBA$_{50\%}$)$_{101}$-*b*-PtBA$_{204}$-*b*-P(nBA$_{50\%}$-*stat*-tBA$_{50\%}$)$_{101}$ triblock copolymer, and (c) acidolysis into TH50.

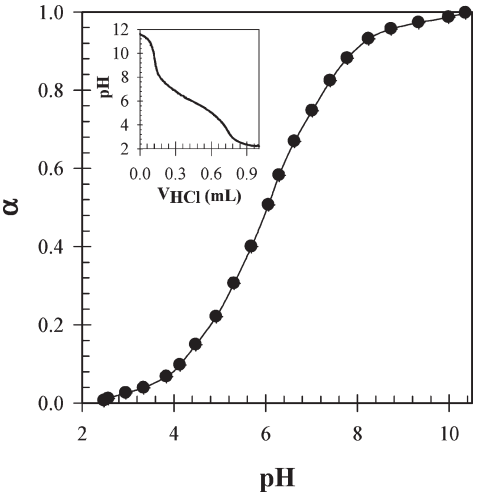

Figure 3. Evolution of α as a function of the pH for a TH50 solution at C = 2.5 g/L. The inset shows the evolution of the pH as a function of the volume of added 1 M HCl.

molecular weight (M_n) and dispersity (M_w/M_n) were determined using polystyrene standards for calibration. It should be noted that this conventional calibration of SEC yields apparent values of M_n, M_w, and dispersity (M_w/M_n).[35] However, the Mark−Houwink−Sakurada (MHS) parameters for PS, PnBA, and PtBA in THF are very similar[36,37] so that the molecular weights and dispersities estimated from SEC may be used to prove the good control of the polymerization.[30,34,38] The molecular weights of the final polymers were calculated from the conversion assuming that termination and transfer reactions were negligible. They are close to the values measured by SEC, as expected given the MHS parameters.

III. RESULTS

1. Synthesis. The P(nBA$_{50\%}$-*stat*-AA$_{50\%}$)$_{101}$-*b*-PAA$_{204}$-*b*-P(nBA$_{50\%}$-*stat*-AA$_{50\%}$)$_{101}$ triblock copolymer, noted henceforth TH50, was synthesized by atom transfer radical polymerization (ATRP). The three-step procedure shown in Figure 2 was similar to what was already reported for a P(nBA$_{50\%}$-*stat*-AA$_{50\%}$)$_{99}$-*b*-PAA$_{98}$ diblock copolymer,[29] except that a difunctional initiator (dimethyl 2,6-dibromoheptandioate)[39] was used instead of a monofunctional one. First, the Br-PtBA$_{204}$-Br difunctional macroinitiator was prepared by polymerization of tBA initiated by dimethyl 2,6-dibromoheptandioate (Figure 2a). The Br-PtBA$_{204}$-Br block (M_n = 2.6 × 10^4 g/mol, M_w/M_n = 1.16) was purified and used to initiate the copolymerization with tBA and nBA to form the two P(nBA$_{50\%}$-*stat*-AA$_{50\%}$)$_{101}$ outer blocks (Figure 2b), yielding a P(nBA$_{50\%}$-*stat*-tBA$_{50\%}$)$_{101}$-*b*-PtBA$_{204}$-*b*-P(nBA$_{50\%}$-*stat*-tBA$_{50\%}$)$_{101}$ triblock copolymer (M_n = 5.2 × 10^4 g/mol, M_w/M_n = 1.10). Finally, the targeted P(nBA$_{50\%}$-*stat*-AA$_{50\%}$)$_{101}$-*b*-PAA$_{204}$-*b*-P(nBA$_{50\%}$-*stat*-AA$_{50\%}$)$_{101}$ (M_n = 3.3 × 10^4 g/mol) was obtained by trifluoroacetic acid-catalyzed elimination of isobutylene from the tBA units of the P(nBA$_{50\%}$-*stat*-tBA$_{50\%}$)$_{101}$-*b*-PtBA$_{204}$-*b*-P(nBA$_{50\%}$-*stat*-tBA$_{50\%}$)$_{101}$ (Figure 2c).

The synthesis of this triblock was very similar to what was already reported for the P(nBA$_{50\%}$-*stat*-AA$_{50\%}$)$_{99}$-*b*-PAA$_{98}$ diblock copolymer;[29] thus, detailed kinetic studies are not presented here. They revealed that the first two ATRP steps proceeded in a controlled manner. The triblock copolymer is narrowly distributed in terms of molecular weight and chemical composition. Moreover, it contains no significant trace of residual Br-PtBA$_{204}$-Br, indicating an efficiency of the macroinitiator close to 100%. Furthermore, copolymerization of tBA and nBA units was purely statistical, leading to a random distribution of these units in the B blocks. Finally, the third step of the synthesis was already shown to be quantitative and selective, implying that it transforms all tBA units into AA without affecting the nBA units or the ester linkages of the difunctional initiator.[30]

2. Potentiometric Titration. A solution of TH50 at C = 2.5 g/L was brought to pH ∼ 11 using an excess of NaOH and subsequently titrated by HCl (inset of Figure 3). The concentration of sodium acrylate units determined by titration[40] was in agreement with the value calculated from the chemical structure of the polymer within the experimental error, indicating that all AA units of the three blocks could be ionized. The ionization of the hydrophilic PAA central block is favored over that of the hydrophobic outer blocks. Nevertheless, AA units, whatever their location, are ionized concomitantly. Their overall degree of ionization (α) was calculated as a function of the pH (see Figure 3). Borukhov et al.[41] showed that titration of polyelectrolytes depends on the polymer concentration at low concentrations. We verified that the results obtained at a higher concentration were the same.

3. Viscosity. Figure 4a shows the evolution of the viscosity relative to that of water (η_r) as a function of the concentration for different ionization degrees at T = 20 °C. For α < 0.3, η_r increased steeply with increasing concentration above a characteristic value of the latter until it became too high to be determined experimentally. For larger α the sharp increase was followed by a much weaker increase at higher concentrations. The latter behavior is expected for transient networks formed by triblock copolymers above the percolation threshold, as was mentioned in the Introduction.

We will define the percolation concentration (C_p) as the concentration where the viscosity starts to increase strongly. Good superposition was obtained when η_r is plotted as a function of C/C_p (see Figure 4b) except at large α where C_p is large and

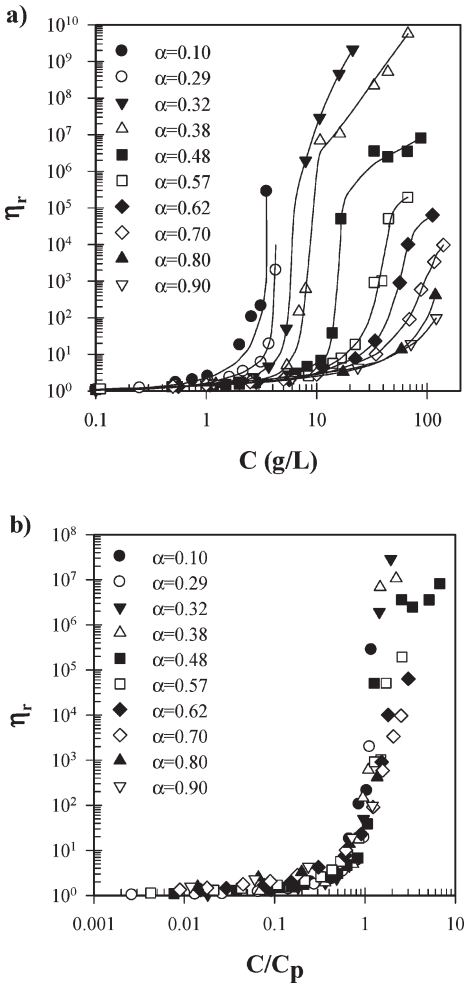

Figure 4. (a) Dependence of the relative viscosity (η_r) of TH50 as a function of the concentration at different ionization degrees (α), at T = 20 °C. The solid lines are guides to the eye. (b) Evolution of η_r as a function of C/C_p at different α.

the viscosity is already significantly increased before the transient network is formed. The dependence of C_p on α is shown in Figure 5. Between α = 0.1 and 0.3, C_p was relatively small and only weakly dependent on α, but at higher ionization degrees C_p increased strongly with increasing α from about 5.5 g/L at α = 0.32 to 100 g/L at α = 0.9.

4. Frequency Dependence of the Shear Moduli. *4.1. Effect of Temperature.* In Figure 6a, the frequency dependences of G' and G'' at temperatures between 20 and 55 °C are plotted for a solution at C = 87 g/L and α = 0.48. At all temperatures, the system behaved as a viscoelastic fluid, demonstrating that the end groups exchanged spontaneously between multiplets. The terminal relaxation time decreased strongly with increasing temperature, but the results at different temperatures could be superimposed using horizontal shift factors (see Figure 6b). Vertical shifts were also used, but they were small for all systems (less than a factor of 2). Comparison with the Maxwell model shows that the transient network studied here was characterized by a broad distribution of relaxation times (see the solid line in Figure 6b).

We will define a characteristic average relaxation time (τ) as the inverse of the radial frequency ($\omega = 2\pi f$) where G' and G'' cross. We found that the temperature dependence of τ could be

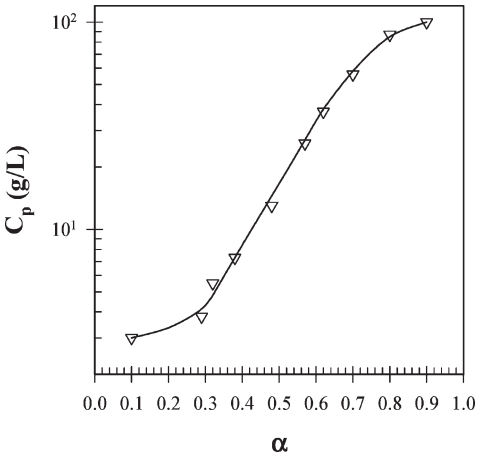

Figure 5. Dependence of the percolation concentration on the ionization degree.

described by the Arrhenius law: $\tau \propto \exp(E_a/RT)$, where R is the gas constant with activation energy $E_a \approx 110$ kJ/mol. The same activation energy was found at all concentrations and ionization degrees where τ could be determined (see Figure 7). The elastic modulus (G_e) was estimated from G' at high frequencies (100 times the crossover frequency).

4.2. Effect of Concentration. In Figure 8a, the frequency dependence of G' and G'' is plotted at concentrations between 16 and 87 g/L at α = 0.48 and 20 °C. Viscoelastic behavior was observed at each concentration. At low concentrations (C < 27 g/L), the elastic modulus increased strongly with increasing concentration, while the relaxation time increased more weakly. At higher concentrations (C > 27 g/L), G' increased more slowly with the concentration and the relaxation time became constant.

We attempted to superimpose the results at different concentrations using horizontal and vertical shift factors. Good superposition could be obtained for the highest concentrations, but not at lower concentrations (see Figure 8b) where the width of the relaxation distribution increased. However, good time−temperature superposition was obtained for a given concentration even at lower concentrations. We will discuss the origin of this phenomenon below. Similar observations were made at other degrees of ionization for α > 0.30. The effect of the concentration and α on G_e and τ (Figures 10 and 11) will be discussed below.

4.3. Effect of Ionization Degree. In Figure 9a, the frequency dependence of the shear moduli is plotted for different α between 0.48 and 0.62 at C = 67 g/L and T = 20 °C. For these values of α, the system behaved as a viscoelastic fluid with a terminal relaxation time that decreased strongly with increasing α. The results could be superimposed using horizontal and vertical shifts and a master curve was obtained with α_{ref} = 0.48 (see Figure 9b). Similar results were obtained at other concentrations. We conclude that results obtained at all temperatures, concentrations, and degrees of ionization could be superimposed to form a single master curve as long as α > 0.30 and the concentration was significantly larger than C_p. The situation at α < 0.30 was quite different and will be discussed below.

5. Elastic Modulus. The concentration dependence of G_e is plotted at different ionization degrees in Figure 10a. For most values of α, G_e increased sharply with increasing concentration starting from C_p followed by a weaker increase at higher concentrations.

dx.doi.org/10.1021/ma2002382 |*Macromolecules* 2011, 44, 4487–4495

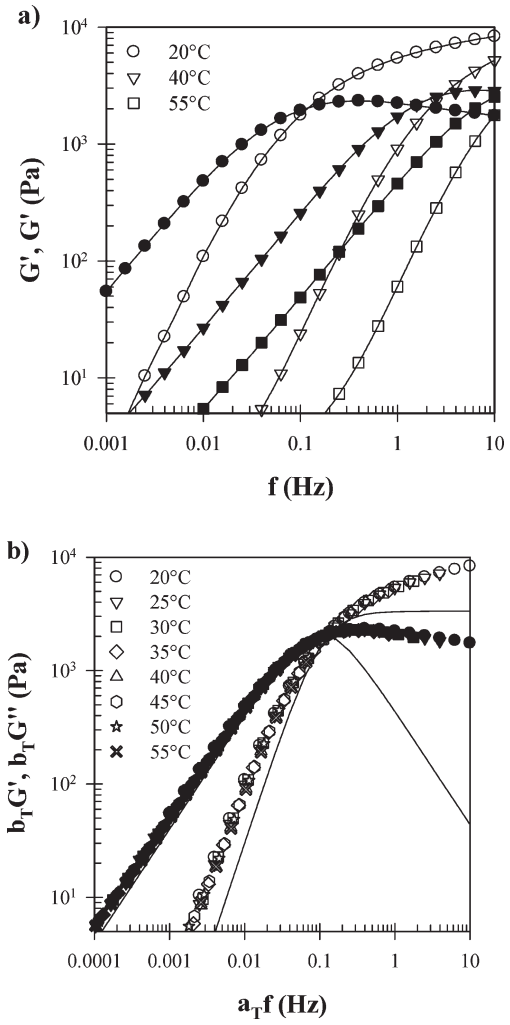

Figure 6. (a) Frequency dependence of the storage (open symbols) and loss (filled symbols) shear moduli at different temperatures for C = 87 g/L and $\alpha = 0.48$. (b) Same data as in (a) after frequency−temperature superposition at T_{ref} = 20 °C. The solid lines represent the Maxwell model.

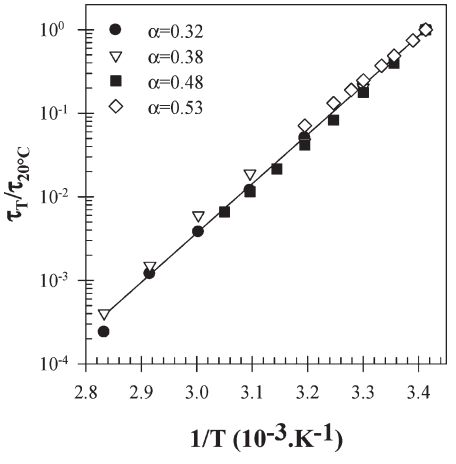

Figure 7. Evolution of τ normalized by its value at 20 °C ($\tau_{20\,°C}$) as a function of $1/T$ and at different ionization degrees. The solid line represents a linear least-squares fit.

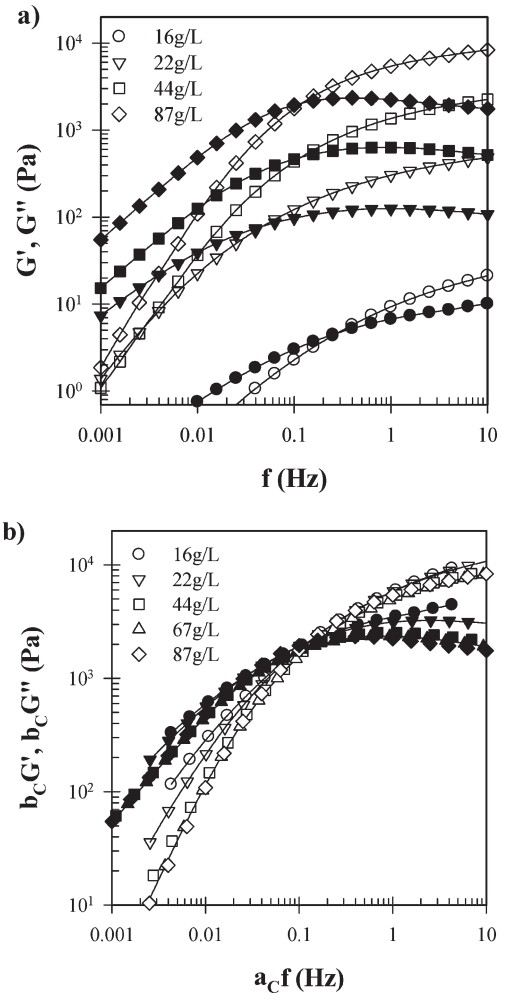

Figure 8. (a) Frequency dependence of the storage (open symbols) and loss (filled symbols) shear moduli at different concentrations at T = 20 °C and $\alpha = 0.48$. (b) Same data as in (a) after frequency−concentration superposition at C_{ref} = 87 g/L. The solid lines are guides to the eye.

However, at $\alpha = 0.32$ and 0.38 the increase was more gradual. If the elasticity is determined purely by the entropy, then $G_e = \nu RT$, where ν is the molar concentration of elastically active network strands.[42] For a fully developed network, all chains are elastically active and $\nu = C/M_n$, where M_n is the number-average molar mass of the polymers. The solid line in Figure 10a shows $G_e = RTC/M_n$, which describes the experimental results obtained at higher concentrations, within the experimental error. The transition from a liquid to a fully formed transient network can be clearly seen if G_e is normalized by RTC/M_n and C by C_p (see Figure 10b). The results are similar in this representation with the exception of those obtained at α = 0.32 and 0.38.

6. Relaxation Time. The dependence of the relaxation time at 20 °C on the degree of ionization is shown in Figure 11 for different concentrations. For $\alpha > 0.30$, τ decreased exponentially over 7 decades (from about 10^4 s to 10^{-3} s) with increasing α up to $\alpha \approx 0.70$ and leveled off at higher ionization degrees. At most ionization degrees there was no systematic effect of the concentration on τ, except very close to C_p. However, we found that τ increased significantly with the concentration at α = 0.38 and even more at α = 0.32.

dx.doi.org/10.1021/ma2002382 |*Macromolecules* 2011, 44, 4487–4495

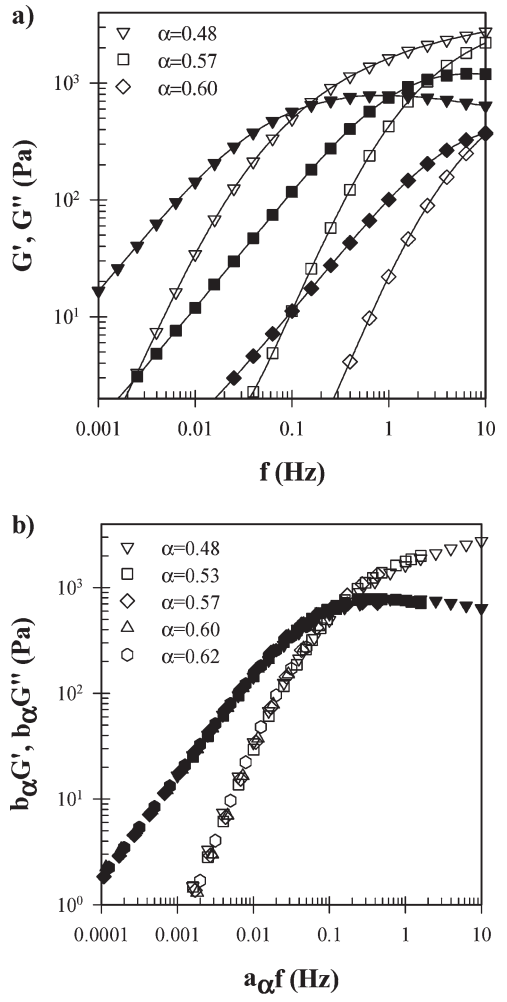

Figure 9. (a) Frequency dependence of the storage (open symbols) and loss (filled symbols) shear moduli and of the relaxation time at C = 67 g/L for TH50 at different α, T = 20 °C. (b) Master curve of the frequency dependence of the storage (open symbols) and loss (filled symbols) shear moduli for systems at C = 67 g/L, α > 0.30, α_{ref} = 0.48.

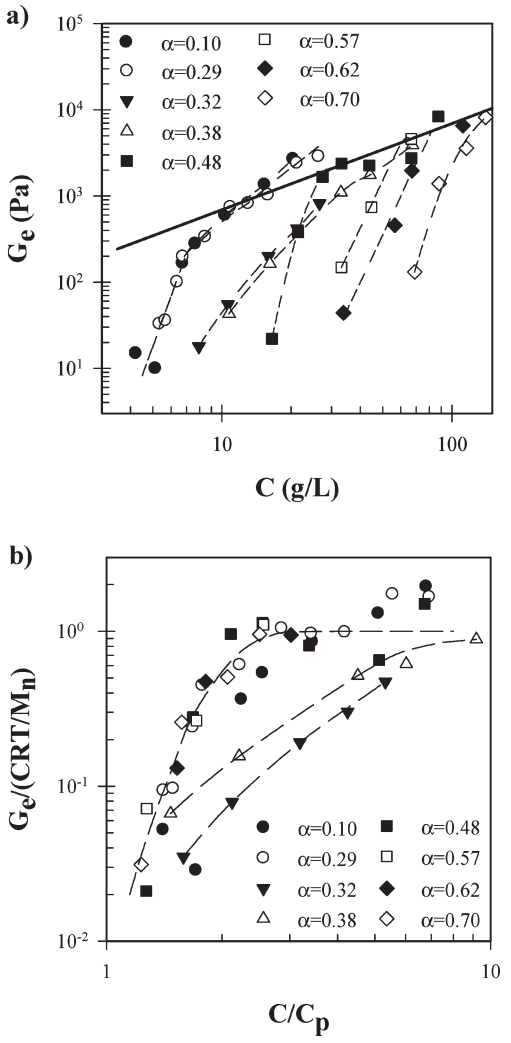

Figure 10. (a) Concentration dependence of G_e for solutions at 0.10 < α < 0.70, T = 20 °C. The dotted lines are guides to the eye whereas the solid line represents the prediction for a fully formed rubber elastic network, i.e., $G_e = CRT/M_n$. (b) Evolution of $G_e/(CRT/M_n)$ as a function of C/C_p at different α. The dotted lines are guides to the eye.

A dramatic slowdown of the relaxation was observed between α = 0.32 and α = 0.29. This is illustrated in Figure 12 which shows master curves of G' and G'' at T_{ref} = 80 °C for ionization degrees between 0.10 and 0.48. The moduli were normalized by G_e in order to facilitate comparison of data that were obtained at different concentrations. Even at this high temperature no crossover was observed at α = 0.29 down to $f = 10^{-3}$ Hz, while at α = 0.32 it occurred at about 0.1 Hz for C = 21 g/L. By comparing the frequency dependence at α = 0.29 with that at α = 0.32 and assuming that the relaxation time distributions are the same, we may estimate that relaxation at α = 0.29 was about 3 orders of magnitude slower than at α = 0.32. Remarkably, the frequency dependence appears to become independent of the ionization degree for α < 0.3.

IV. DISCUSSION

The rheology of TH50 shows that for α ≥ 0.32 the self-assembly of this polymer is dynamic. This result is in stark contrast with the behavior of block copolymers consisting of pure PAA and P*n*BA blocks that form frozen aggregates in aqueous solution.[17,27] We thus demonstrated that incorporating hydrophilic units into the hydrophobic block(s) of an amphiphilic block copolymers can transform a frozen system into a dynamic one.

In addition, the associative polymer system described here has the originality that its rheology can be controlled by the pH due to the introduction of the right amount of hydrophilic, pH-sensitive AA monomers into the hydrophobic block. Remarkably, the same solutions showed both the behavior of kinetically frozen and dynamic triblock copolymers at low and high pH, respectively. The transition between these two kinds of behavior occurs over a small range of α between 0.29 and 0.32. We will first discuss the behavior of the dynamic systems at ionization degrees above 0.32 and then speculate on the features of the frozen system at smaller values of α.

1. Dynamic Systems. In aqueous solution at α ≥ 0.32 the hydrophobic end-blocks of the triblock copolymers associated into multiplets, whereas the hydrophilic central block either formed loops or bridged two multiplets. Bridging led to aggregation of the multiplets and above a critical concentration to the

dx.doi.org/10.1021/ma2002382 |*Macromolecules* 2011, 44, 4487–4495

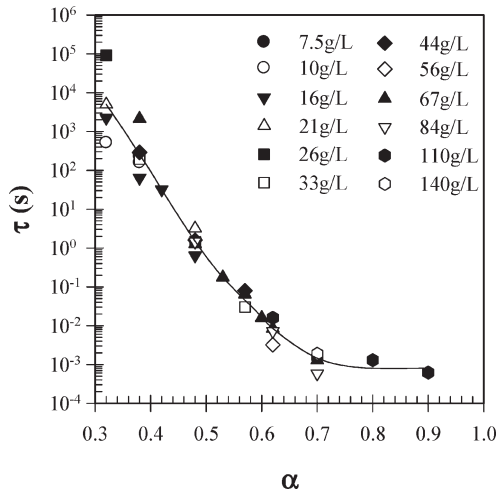

Figure 11. Evolution of the average relaxation time as a function of the ionization degree at different concentrations, $T = 20$ °C. The solid line is a guide to the eye.

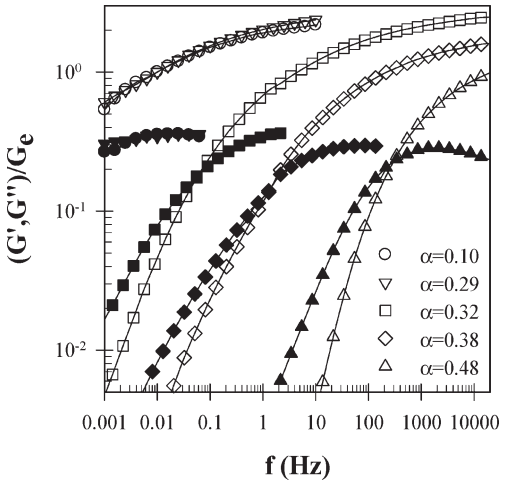

Figure 12. Master curves of the normalized storage (open symbols) and loss (filled symbols) shear moduli with $T_{ref} = 80$ °C for different degrees of ionization indicated in the figure. For clarity, not all data points are shown.

formation of a system spanning, percolating network.[7−9] A consequence of the formation of a transient network was that the viscosity started to increase sharply, and the system responded elastically to deformation at high oscillation frequencies. Close to the percolation concentration the elastic modulus measured at high frequencies was small, because only a small fraction of the polymers was part of the network and the network itself contained many defects. With increasing concentration an increasing fraction of chains were integrated into the network and the amount of defects decreased, which led to an increase of G_e.[43] Defects of the network also explain why the relaxation time distribution was broader and τ was smaller close to C_p. At high concentrations the amount of defects became negligibly small, and the elastic modulus was close to that expected for an ideal rubber-elastic network where all chains are elastically active.[42]

The behavior described above was earlier studied in detail for PEO end-capped with (fluoro)alkyl groups.[3,5,11,44] For these systems the terminal relaxation of the shear modulus is characterized by a single well-defined relaxation time contrary to the system investigated here, which showed a broad distribution of relaxation times. Broad relaxation distributions have earlier been observed for systems with longer and less mobile hydrophobic blocks.[6,9,45]

Relaxation of the shear modulus occurs by escape of a bridging hydrophobic group from a multiplet, which may schematically be described in three steps: (1) retraction of the chain to the interface with the corona; (2) entering of the corona; (3) diffusion through the corona.[13,46] A single relaxation time implies that the escape rate is determined by a single rate-limiting process, which is generally thought to be step 2. However, when the diffusion of the chains is restricted, step 1 may become rate-limiting, which leads to a broad distribution of relaxation times. A different possible origin of a broad relaxation process is the polydispersity of the hydrophobic blocks in both length and composition, regardless of whether step 1 or step 2 is rate-limiting.

The energy barrier that the hydrophobic block has to overcome to exit the core and enter the corona is proportional to the interfacial tension between the core and the corona as well as to the length of the hydrophobic block.[13,25] Therefore, the relaxation time increases with increasing hydrophobicity of the associating block. This explains for instance the strong increase of τ with increasing length of the hydrophobic group and the increase that is observed if normal alkyl is replaced by fluorinated alkyl.[5,11] However, for a range of systems an Arrhenius temperature dependence was observed with similar activation energies to that observed here[4,47−51] in spite of the fact that the terminal relaxation times were very different. Here we have found for the same system a strong variation of the relaxation time with α, but nevertheless the same activation energy. Clearly, the absolute exchange rate of end groups between multiplets is not correlated to the activation energy that appears in the Arrhenius equation.

The most striking feature of the system studied here was the exponential decrease of the relaxation time with decreasing ionization degree between α = 0.32 and 0.7. The implication is that the energy barrier for the escape of an end-block decreases linearly with the charge density in this range. Interestingly, while the relaxation time varied by about 7 orders of magnitude, the width of the relaxation time distribution remained the same. This suggests that the escape of the end-blocks is rate limited by step 2 and that the broad relaxation time distribution is a consequence of the polydispersity that does not change with α. At larger ionization degrees the relaxation time no longer depended strongly on α, indicating that either the effective charge density no longer increased due to counterion condensation or that a further increase of the electrostatic interaction no longer strongly influenced the escape process.

Not only the relaxation but also the propensity to form a system spanning network depended on α. The percolation concentration increased with increasing α and reached values as high as 100 g/L at α = 0.9 (see Figure 5). At such high concentrations, the polymer chains started to overlap, and one may argue that the increase of the viscosity could be caused by entanglements. However, the viscosity of pure PAA chains with higher molar mass is much smaller,[52] and we may therefore safely conclude that even at α = 0.9 the chains associate at sufficiently high concentrations. The increase of C_p with increasing α may have several causes. If the aggregation number increases with

dx.doi.org/10.1021/ma2002382 |*Macromolecules* 2011, 44, 4487–4495

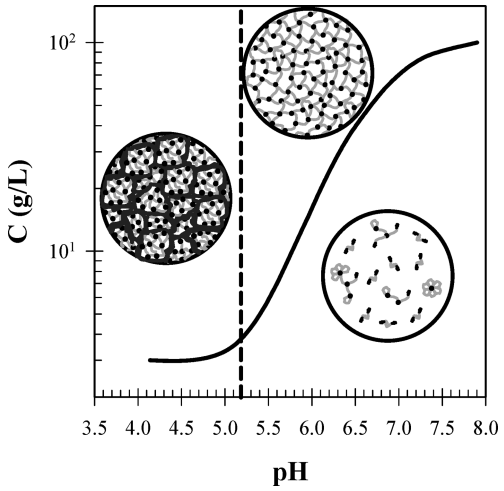

Figure 13. State diagram of the concentration versus the pH for TH50. The solid line indicates the percolation concentration, and the dotted line indicates the transition between frozen and dynamic assemblies at lower pH and higher pH, respectively. The drawings are schematic representations of the systems in different regions of the state diagram (see text).

increasing α, fewer multiplets are formed so that more polymer is needed to fill up the space. However, this is counterintuitive as the polymer becomes more charged and thus less hydrophobic at higher α. Moreover, an investigation of the corresponding diblocks referred to in the Introduction showed that the aggregation number decreased with increasing α.[29] A second possibility is that the corona size decreases with increasing α. This is also unlikely since the charge density of the corona increases with increasing α, and thus one would expect, if anything, that the corona increases in size with increasing α. The remaining explanation is that the fraction of polymers that associates at a given concentration decreases with increasing α.

For a monodisperse diblock or triblock copolymer, association is a cooperative process akin to micellization of surfactants that starts at a critical association concentration (CAC). CAC depends on the hydrophobicity of the B blocks[53,54] and is therefore expected to increase with increasing α. For a polydisperse system the transition is more gradual, but still with increasing concentration an increasing fraction of the polymers associates.[55,56] Indeed, in spite of a well-controlled synthesis the TH50 chains are somewhat polydisperse in both molar mass and chemical composition. The increase of C_p with increasing α can thus be understood by the increase of the association concentration. At sufficiently high polymer concentrations most polymers are associated and elastically active for all values of α.

2. Frozen Systems. For $\alpha \leq 0.29$ no flow behavior was observed for $C > C_p$ in oscillating shear measurements down to 10^{-3} Hz even at 80 °C, and the viscosity was immeasurably large. By comparing the frequency dependence of the shear moduli of these systems with that at larger α, we may estimate $\tau = 10^7$ s at 20 °C, assuming that the activation energy remains the same. Thus, on the time scales that are experimentally accessible these systems were frozen with negligible exchange of end-blocks between multiplets. Nevertheless, the elastic modulus was comparable within experimental error to that expected for a rubber-elastic network. When the systems were forced to flow, they showed strong shear thinning, but after cessation of flow, gel-like behavior was recovered immediately. Similar behavior has been reported for other triblock copolymers that did not show a measurable relaxation time.[21−24,57−59]

For not too high concentrations, homogeneous perfectly transparent gels could be obtained within a day even below $\alpha = 0.3$, which means that we can exclude that a network is formed by very slow exchange of end-groups. In addition, when the gel is loaded onto the rheometer, a system spanning network is necessarily broken up. Nevertheless, the response was elastic over the whole frequency range immediately after loading. The rapid recovery after cessation of shear flow also shows that the system is elastic before the network had time to heal. This behavior can be explained by considering that the network is broken up into a suspension of close-packed microgels. When small oscillatory stress is applied, the stress is carried by the microgels. The elastic modulus of such a system is therefore not expected to be very different from the unperturbed network in the linear response regime.

The question remains why the relaxation does not continue to slow down exponentially with decreasing α, but becomes practically arrested at $\alpha \approx 0.3$. We have as yet no answer to this question and can only speculate that below this ionization degree a different, much stronger, type of interaction between the hydrophobic blocks occurs. Possibly, the strong increase of the relaxation time observed for $\alpha = 0.32$ at higher concentrations is also due to a transition between the two types of behavior. A better understanding of this transition can perhaps be obtained by varying the fraction of AA segments in the hydrophobic block. We have observed that P(*n*BA-*stat*-AA)-*b*-PAA diblocks containing 80 mol % AA units in the hydrophobic block instead of 50 mol % self-assemble more weakly.[28] Therefore, we expect that increasing the fraction of AA segments will lead to a decrease of the relaxation time at a given pH and to a systematic shift of the pH dependence of τ to lower pH. Thus, by simply varying the fraction of AA segments, it will be possible to adjust the strongly pH-dependent rheology to different pH ranges.

V. CONCLUSIONS

Triblock BAB copolymers can form a system spanning network by self-assembly above a critical percolation concentration. For many aqueous systems exchange of B-blocks is extremely slow so that the structure is frozen on experimental time scales. Here we have demonstrated for the first time that the association can be rendered dynamic by incorporating hydrophilic monomers into the hydrophobic end blocks. In addition, we showed that by introducing acidic units the dynamics and thus the rheological properties of the system can be fine-tuned and controlled by the pH.

For TH50 a transition was observed with increasing pH between frozen hydrogels at pH < 5.2 and viscoelastic solutions at higher pH. The terminal relaxation time and thus the viscosity decreases sharply with increasing pH. In the state diagram of the polymer concentration versus the pH we may distinguish four regions (see Figure 13). For $C > C_p$ and pH > 5.2 ($\alpha > 0.3$), the polymers form a transient network and the system behaves as a viscoelastic liquid with a viscosity that strongly depends on the pH and *C*. For $C < C_p$ and pH > 5.2 ($\alpha > 0.30$), the solutions contain free polymers, micelles, and clusters of micelles and the viscosity is low except close to C_p. For $C > C_p$ and pH < 5.2 ($\alpha < 0.30$), the system is dynamically frozen and behaves as an elastic solid on the time scales of the experiment. It probably consists of

densely packed microgels. Finally, for $C < C_p$ and pH < 5.2 ($\alpha <$ 0.30) the system forms a very low-viscosity liquid containing aggregates. Notice that the line separating frozen from dynamic systems is not necessarily exactly vertical.

AUTHOR INFORMATION

Corresponding Author

*E-mail: christophe.chassenieux@univ-lemans.fr (C.C.), olivier.colombani@univ-lemans.fr (O.C.).

ACKNOWLEDGMENT

This work has been funded by the Agence Nationale de la Recherche in the framework ANR-09-BLAN-0174-01. The authors thank Magali Martin for the SEC analysis.

REFERENCES

(1) Bossard, F.; Tsitsilianis, C.; Yannopoulos, S. N.; Petekidis, G.; Sfika, V. *Macromolecules* **2005**, *38*, 2883–2888.

(2) Bossard, F.; Aubry, T.; Gotzamanis, G.; Tsitsilianis, C. *Soft Matter* **2006**, *2*, 510–516.

(3) Tam, K. C.; Jenkins, R. D.; Winnik, M. A.; Bassett, D. R. *Macromolecules* **1998**, *31*, 4149–4159.

(4) Séréro, Y.; Aznar, R.; Porte, G.; Berret, J. F. *Phys. Rev. Lett.* **1998**, *81*, 5584–5587.

(5) Pham, Q. T.; Russel, W. B.; Thibeault, J. C.; Lau, W. *Macromolecules* **1999**, *32*, 5139–5146.

(6) Seitz, M. E.; Burghardt, W. R.; Faber, K. T.; Shull, K. R. *Macromolecules* **2007**, *40*, 1218–1226.

(7) Winnik, M. A.; Yekta, A. *Curr. Opin. Colloid Interface Sci.* **1997**, *2*, 424–436.

(8) Annable, T.; Buscall, R.; Ettelaie, R.; Shepherd, P.; Whittlestone, D. *Langmuir* **1994**, *10*, 1060–1070.

(9) Chassenieux, C.; Nicolai, T.; Benyahia, L. *Curr. Opin. Colloid Interface Sci.* **2011**, *16*, 18–26.

(10) Larson, R. G. *The Structure and Rheology of Complex Fluids*; Oxford University Press: New York, 1999.

(11) Berret, J. F.; Calvet, D.; Collet, A.; Viguier, M. *Curr. Opin. Colloid Interface Sci.* **2003**, *8*, 296–306.

(12) Renou, F.; Nicolai, T.; Nicol, E.; Benyahia, L. *Langmuir* **2009**, *25*, 515–521.

(13) Nicolai, T.; Colombani, O.; Chassenieux, C. *Soft Matter* **2010**, *6*, 3111–3118.

(14) Popescu, M.-T.; Athanasoulias, I.; Tsitsilianis, C.; Hadjiantoniou, N. A.; Patrickios, C. S. *Soft Matter* **2010**, *6*, 5417–5424.

(15) Zana, R.; Marques, C.; Johner, A. *Adv. Colloid Interface Sci.* **2006**, *123−126*, 345–351.

(16) Meli, M.; Lodge, T. P. *Macromolecules* **2009**, *42*, 580–583.

(17) Colombani, O.; Ruppel, M.; Burkhardt, M.; Drechsler, M.; Schumacher, M.; Gradzielski, M.; Schweins, R.; Müller, A. H. E. *Macromolecules* **2007**, *40*, 4351–4362.

(18) Bendejacq, D.; Joanicot, M.; Ponsinet, V. *Eur. Phys. J. E* **2005**, *17*, 83–92.

(19) Petrov, P. D.; Drechsler, M.; Müller, A. H. E. *J. Phys. Chem. B* **2009**, *113*, 4218–4225.

(20) Théodoly, O.; Jacquin, M.; Muller, P.; Chhun, S. *Langmuir* **2009**, *25*, 781–793.

(21) Tsitsilianis, C.; Iliopoulos, I.; Ducouret, G. *Macromolecules* **2000**, *33*, 2936–2643.

(22) Tsitsilianis, C.; Iliopoulos, I. *Macromolecules* **2002**, *35*, 3662–3667.

(23) Stavrouli, N.; Aubry, T.; Tsitsilianis, C. *Polymer* **2008**, *49*, 1249–1256.

(24) Angelopoulos, S. A.; Tsitsilianis, C. *Macromol. Chem. Phys.* **2006**, *207*, 2188–2194.

(25) Halperin, A.; Alexander, S. *Macromolecules* **1989**, *22*, 2403–2412.

(26) Stam, J. V.; Creutz, S.; De Schryver, F. C.; Jérôme, R. *Macromolecules* **2000**, *33*, 6288–6395.

(27) Jacquin, M.; Muller, P.; Talingting-Pabalan, R.; Cottet, H.; Berret, J. F.; Futterer, T.; Théodoly, O. *J. Colloid Interface Sci.* **2007**, *316*, 897–911.

(28) Lejeune, E.; Chassenieux, C.; Colombani, O. *Prog. Colloid Polym. Sci.* (DOI 10.1007/978-3-642-19038-4_2).

(29) Lejeune, E.; Drechsler, M.; Jestin, J.; Müller, A. H. E.; Chassenieux, C.; Colombani, O. *Macromolecules* **2010**, *43*, 2667–2671.

(30) Colombani, O.; Ruppel, M.; Schubert, F.; Zettl, H.; Pergushov, D. V.; Müller, A. H. E. *Macromolecules* **2007**, *40*, 4338–4350.

(31) Dimitrova, I.; Trzebickab, B.; Müller, A. H. E.; Dworak, A.; Tsvetanova, C. B. *Prog. Polym. Sci.* **2007**, *32*, 1275–1343.

(32) Bütün, V.; Liu, S.; Weaver, J. V. M.; Bories-Azeau, X.; Cai, Y.; Armes, S. P. *React. Funct. Polym.* **2006**, No. 66, 157–165.

(33) Arotçaréna, M.; Heise, B.; Ishaya, S.; Laschewsky, A. *J. Am. Chem. Soc.* **2002**, *124*, 3787–3793.

(34) Colombani, O.; Langelier, O.; Martwong, E.; Castignolles, P. *J. Chem. Educ.* **2011**, *88*, 116–121.

(35) Grubisic, Z.; Rempp, P.; Benoit, H. *J. Polym. Sci., Part B: Polym. Phys.* **1996**, *34*, 1707–1713.

(36) Beuermann, S.; Paquet, D. A. J.; McMinn, J. H.; Hutchinson, R. A. *Macromolecules* **1996**, *29*, 4206–4215.

(37) Castignolles, P.; Graf, R.; Parkinson, M.; Wilhelm, M.; Gaborieau, M. *Polymer* **2009**, *50*, 2373–2383.

(38) Guillaneuf, Y.; Castignolles, P. *J. Polym. Sci., Part A: Polym. Chem.* **2008**, *46*, 897–911.

(39) Davis, K. A.; Charleux, B.; Matyjaszewski, K. *J. Polym. Sci., Part A: Polym. Chem.* **2000**, *38*, 2274–2283.

(40) Bendejacq, D. D.; Ponsinet, V. *J. Phys. Chem. B* **2008**, *112*, 7996–8009.

(41) Borukhov, I.; Andelman, D.; Borrega, R.; Cloitre, M.; Leibler, L.; H., O. *J. Phys. Chem. B* **2000**, *104*, 11027–11034.

(42) Green, M. S.; Tobolsky, A. V. *J. Chem. Phys.* **1946**, *14*, 80–92.

(43) Annable, T.; Buscall, R.; Ettelaie, R.; Whittlestone, D. *J. Rheol.* **1993**, *37*, 695–726.

(44) Tae, G.; Kornfield, J. A.; Hubbell, J. A.; Lal, J. *Macromolecules* **2002**, *35*, 4448–4457.

(45) Lund, R.; Willner, L.; Richter, D.; Iatrou, H.; Hadjichristidis, N.; Lindner, P. *J. Appl. Crystallogr.* **2007**, *40*, s327–s331.

(46) Tian, M.; Qin, A.; Ramireddy, C.; Webber, S. E.; Munk, P.; Tuzar, Z.; Prochazka, K. *Langmuir* **1993**, *9*, 1741–1748.

(47) Séréro, Y.; Jacobsen, V.; Berret, J. F. *Macromolecules* **2000**, *33*, 1841–1847.

(48) Wang, J.; Benyahia, L.; Chassenieux, C.; Tassin, J. F.; Nicolai, T. *Polymer* **2010**, *51*, 1964–1971.

(49) Petit, F. Thesis University Paris 6, Paris, 1996.

(50) Bednar, B.; Karasek, L.; Pokorny, J. *Polymer* **1996**, *37*, 5261–5268.

(51) Wang, Y.; Kausch, C. M.; Chun, M.; Quirk, R. P.; Mattice, W. L. *Macromolecules* **1995**, *28*, 904–911.

(52) Perrin, P.; Lafuma, F. *J. Colloid Interface Sci.* **1998**, *197*, 317–326.

(53) Alexandridis, P.; Hatton, T. A. *Colloids Surf., A* **1995**, *96*, 1–46.

(54) Jacquin, M.; Muller, P.; Cottet, H.; Théodoly, O. *Langmuir* **2010**, *26*, 18681–18693.

(55) Gao, Z.; Eisenberg, A. *Macromolecules* **1993**, *26*, 7353–7360.

(56) Nilsson, M.; Håkansson, B.; Soderman, O.; Topgaard, D. *Macromolecules* **2007**, *40*, 8250–8258.

(57) Castelletto, V.; Hamley, I. W.; Ma, Y.; Bories-Azeau, X.; Armes, S. P. *Langmuir* **2004**, *20*, 4306–4309.

(58) He, Y.; Boswell, P. G.; Bühlmann, P.; Lodge, T. P. *J. Phys. Chem. B* **2007**, *111*, 4645–4652.

(59) Hietala, S.; Nuopponen, M.; Kalliomäki, K.; Tenhu, H. *Macromolecules* **2008**, *41*, 2627–2631.